Title

Electron-positron pair creation in the electric fields generated by micro-bubble implosions

Journal

Physics Letters A, 384(34)

ISSN

0375-9601

Authors

Koga, James K

Murakami, Masakatsu

Arefiev, Alexey V

et al.

Publication Date

2020-12-01

DOI

10.1016/j.physleta.2020.126854

Peer reviewed

Electron-Positron Pair Creation in the Electric Fields Generated by Micro-bubble Implosions

James K. Koga[a,*], Masakatsu Murakami[b], Alexey V. Arefiev[c], Yoshihide Nakamiya[d], Stepan S. Bulanov[e], Sergei V. Bulanov[a,f]

[a] *Kansai Photon Science Institute, National Institutes for Quantum and Radiological Science and Technology, Kizugawa, Kyoto 619-0215, Japan*
[b] *Institute of Laser Engineering, Osaka University, Osaka, 565-0871, Japan*
[c] *Department of Mechanical and Aerospace Engineering, University of California at San Diego, La Jolla, CA 92093, USA*
[d] *Extreme Light Infrastructure-Nuclear Physics (ELI-NP) / Horia Hulubei National Institute for R&D in Physics and Nuclear Engineering (IFIN-HH), 30 Reactorului St., Bucharest-Magurele, jud. Ilfov, P.O.B. MG-6, RO-077125, Romania*
[e] *Lawrence Berkeley National Laboratory, Berkeley, California 94720, USA*
[f] *Institute of Physics ASCR, v.v.i. (FZU), ELI BEAMLINES, Za Radnicí 835, Dolní Břežany 25241, Czech Republic*

Abstract

We show that electron-positron pair production from the vacuum is possible via the strong Coulomb fields generated by micro-bubble implosions induced by ultra-high intensity lasers. Even in the case where the Coulomb fields are lower than the pair creation threshold, externally injected high energy electrons or photons could be used to generate pairs.

Keywords: pair creation, vacuum, micro-bubble implosion, ultra-high intensity lasers

1. Introduction

One of the early predictions of quantum electrodynamics (QED) was the possibility of the production from vacuum of electron-positron pairs via sufficiently strong electric fields[1, 2, 3]. One way of achieving such strong fields is via ultra-high intensity lasers. The peak

*Corresponding author
Email address: koga.james@qst.go.jp (James K. Koga)

laser intensity has risen rapidly since the invention of chirped pulse amplification (CPA) [4]. **Peak intensities of** 10^{22} **W/cm**^{2} **[5, 6],** $\sim 2 \times 10^{22}$ **W/cm**^{2}**[7] and** 5.5×10^{22} **W/cm**^{2} **[8] have been achieved. Higher intensities,** $\sim 10^{23}$ **W/cm**^{2}**, are expected at current/near future facilities such as the extreme light infrastructurenuclear physics (ELI-NP) [9], ELI-beamlines[10] and Apollon [11]. Even higher intensities,** $> 10^{23}$ **W/cm**^{2}**, are anticipated at proposed future laser facilities such as Station of Extreme Light (SEL)[12, 13] and others (see review [14]).** However, the peak laser intensities even at the future laser facilities will be orders of magnitude below the **Schwinger field,** E_S**,** required to breakdown the vacuum [1, 2, 3]:

$$E_S = \frac{m_e^2 c^3}{e\hbar} = 1.32 \times 10^{18} \text{V/m} \tag{1}$$

or the equivalent intensity of $I_S = 2.3 \times 10^{29}$ W/cm^2 where m_e is the electron mass, c is the speed of light in vacuum, e is the electron charge and $\hbar$ is Planck's constant.

One way to induce vacuum breakdown is by simultaneously focusing multiple colliding laser pulses (MCLPs) where it has been found that the electron-positron pair production threshold could be substantially reduced due to localization of their electromagnetic energy into a smaller volume compared to single or double pulses and the favoring of the electric field [15, 16, 17]. Additionally, the collision of electron beams with MCLPs along with a source of high energy photons [18] has been found to have a regime of efficient pair production at sufficiently high laser power and electron energies [19].

Another way of achieving very strong electrostatic fields is through micro-bubble implosions [20]. It has been proposed as a novel way to approach the Schwinger field [21]. **In figure 1 we show a schematic of the sequence of the micro-bubble implosion.** We have previously shown that these fields are strong enough to deflect gamma-rays passing nearby them [22]. Here, we look into the generation of electron-positron pairs from the vacuum in such a system.

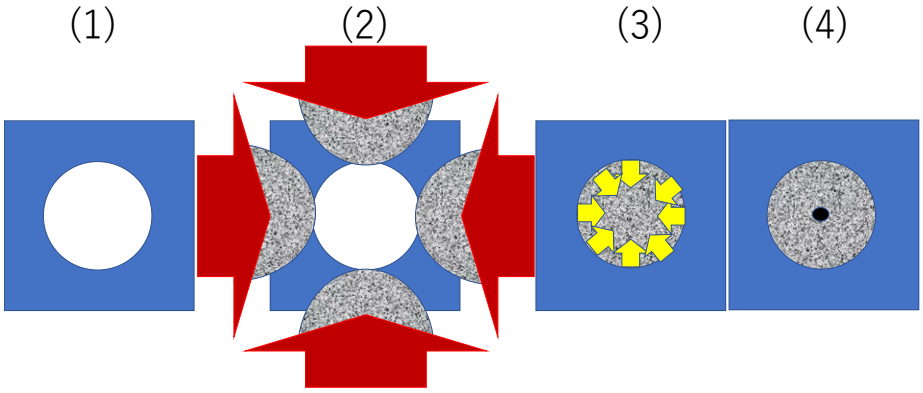

Figure 1: Schematic of the sequence of the micro-bubble implosion: (1) a hollow spherical cavity in a solid material (blue region), (2) irradiation of the surface of the material by ultra-high intensity lasers producing hot electrons streaming from the surface (grey areas) into the cavity, (3) the cavity is filled with these hot electrons which results in an electric field at the surface of the cavity walls (yellow arrows), which pulls the ions in the solid towards the center of the cavity, and (4) the ions converge at the center of the cavity producing a ultrahigh density core (black circle) with a large electrostatic field.

2. Micro-bubble Electric field

In the micro-bubble implosion a solid with a spherical empty cavity is irradiated by an ultra-intense laser producing hot electrons which are generated according to ponderomotive scaling[23]. The hot electron temperature could be enhanced over the pondermotive scaling, however, when the pulse duration is optimal **[24, 25]**. With laser intensities of the order of $10^{21} - 10^{23}$ W/cm^2 this can lead to temperatures ranging from $10 - 100$ MeV [21]. These electrons fill the cavity generating uniform electrostatic fields inside and outside the cavity driving a spherically uniform implosion[20, 21]. It has been shown with a simple 1D model that the maximum electric field, E_{max}, at maximum compression is [21]:

$$E_{max} = \frac{Q_0}{8R_0 r_{min}} \tag{2}$$

where $r_{min} = 3n_{i0}^{2/3}/\tilde{n}_{e0}$ is the minimum radius of the implosion, R_0 and $Q_0 = eN_{e0}$ are the initial radius of and total initial electron charge in the micro-bubble

where the number of electrons is given by $N_{e0} = (4\pi/3)R_0^3\tilde{n}_{e0}$, $\tilde{n}_{e0}$ **is the average electron density after the initially empty micro-bubble has been homogeneously filled up with high energy electrons accelerated by the ultrahigh intensity lasers at the target surface**, e is the electron charge and n_{i0} is the initial ion density of the solid being irradiated. Plugging these equations into Eq. 2 and simplifying we get:

$$E_{max} = \frac{\pi e}{18}\frac{(\tilde{n}_{e0}R_0)^2}{n_{i0}^{2/3}} \tag{3}$$

Typical parameters from [20] assuming that solid hydrogen is irradiated are $n_{i0} = 5 \times 10^{22}\text{cm}^{-3}$, $\tilde{n}_{e0} = 5 \times 10^{21}\text{cm}^{-3}$, and $R_0 = 2\mu$m. The resulting minimum radius is $r_{min} = 8.14$ nm at maximum compression. **Three dimensional molecular dynamics simulations of the innermost protons, which precisely take into account binary collisions, have shown that random collisions scatter the protons around the minimum radius with a substantial fraction compressed into an even smaller central volume[21].** The ratio of the maximum electric field to the Schwinger field is $E_{max}/E_S \approx 1.4 \times 10^{-3}$ (1.8×10^{15} V/m). Fields around this order could deflect gamma-rays up to milli-radian levels passing near the imploded core [22].

Given these typical parameters we can roughly estimate the type of laser which would be required to achieve the implosion. The required intensity is determined by R_0^* in the limiting case of full ionization of the target, $\alpha = 1$, where the ion Debye length is taken to be 2.5 times R_0[21]: $R_0^*(\mu\text{m}) \approx 0.55(I_{L22}\lambda_{L\mu}^2)^{1/4}\alpha^{-1/2}$ where I_{L22} is the laser intensity in units of 10^{22} W/cm^2 and $\lambda_{L\mu}$ is the laser wavelength in μm. Assuming that the laser spot is $R_0 = 2\mu$m we get a laser intensity of $I = 1.74 \times 10^{24}\text{W/cm}^2$ taking $\lambda_{L\mu} = 1$. **We have chosen the laser spot size to be the radius of the bubble, however, the spot could be larger or smaller depending on how the electrons propagate from the interaction region at the target surface, which requires further detailed investigation.** The corresponding laser power is $P_L = \pi R_0^2 I/2 = 109\text{PW}$. The laser pulse duration would be on the order of the characteristic timescale of the bubble implosion $\tau \sim 2\pi/\omega_{pi} \approx 20$fs [21] where

$\omega_{pi} = \sqrt{4\pi e^2 n_{i0}/m_i}$ with m_i being the proton mass is the ion plasma frequency. Therefore, the corresponding laser energy $E_L \approx P_L \tau \sim 2$kJ. **Such lasers of this order are being planned [12, 13, 14].** However, achieving a uniform distribution of hot background electrons will most likely require multiple lasers. **Two dimensional particle-in-cell (PIC) simulations performed with a single bubble implosion in a square target showed that flat lasers normally irradiating in the four directions of the square accelerated electrons quickly filling the bubble rather uniformly and that the electric field around the imploding bubble kept its circular shape[20]. Although more detailed analysis is necessary this would imply** uniform irradiation would require 6 directions in 3D. **Allowing the ion Debye length to be 6 times smaller than R_0 we can take the laser intensity to be $I = 5\times10^{22}$ W/cm^2 still achieving maximum fields $E_{max}/E_S \approx 3\times10^{-3}$ (3.8×10^{15} V/m). Assuming that we are irradiating a sphere with radius $3R_0$ where $R_0 = 2\mu m$ the total required power would be $4\pi(3R_0)^2 I \simeq 226$ PW. Dividing this by 6 beams we get $\simeq 38$ PW per beam or 760 J assuming 20 fs for the duration of the beam. A common feature of future planned > 200 PW laser systems is that multiple beams are coherently combined due to single beam delivery constraints [14]. This could be favorable for achieving an uniform electron distribution and reduction in the required power.**

In Fig. 2 using these typical parameters of the micro-bubble implosion we plot E_{max}/E_S obtained **from Eq. 3** by (a) varying $\tilde{n}_{e0}$ keeping R_0 fixed and (b) varying R_0 keeping $\tilde{n}_{e0}$ fixed. From this figure and Eq. 3, $E_{max} \propto (\tilde{n}_{e0} R_0)^2$. Although varying $\tilde{n}_{e0}$ and R_0 have the same proportionality factors, increasing E_{max} via increasing $\tilde{n}_{e0}$ may be easier than increasing R_0. From the scaling of the maximum electric field versus laser intensity it was shown that a larger R_0 requires a correspondingly larger laser intensity [21]. However, it has been proposed that at the same laser intensity the upper limit on the maximum field could be increased by coating the target surface with a high-Z material or using a hydride such as plastic (CH) to increase the absolute number of

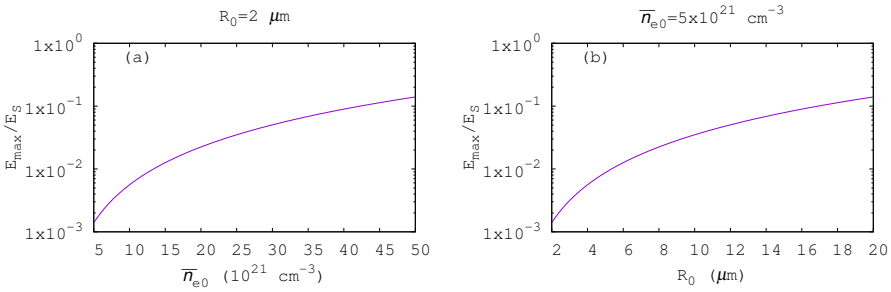

Figure 2: Ratio of the maximum electric field in a micro-bubble implosion at maximum compression **obtained from Eq. 3** to the Schwinger field, E_{max}/E_S, varying (a) the initial average electron density, $\tilde{n}_{e0}$, keeping R_0 fixed and (b) the initial radius of the bubble, R_0, keeping $\tilde{n}_{e0}$ fixed with the typical parameters of $n_{i0} = 5 \times 10^{22}\text{cm}^{-3}$, $\tilde{n}_{e0} = 5 \times 10^{21}\text{cm}^{-3}$, and $R_0 = 2\mu$m.

hot electrons initially in the bubble, $\tilde{n}_{e0}$ [21]. Gold (Au) could be another excellent material to substantially increase $\tilde{n}_{e0}$ and, therefore, N_{e0}. **Maximum electric fields approaching the Schwinger field, for example 10% of the Schwinger field, could be achieved with the same power laser as estimated above by simply increasing the initial number of hot electrons so that $\tilde{n}_{e0} \approx 4 \times 10^{22}\mathbf{cm}^{-3}$.**

Given these fields we examine the pair production possibilities in the next section.

3. Pair creation

An electromagnetic field extending over a finite volume and time will produce a total average number of pairs, N, given by [2, 3] and [26, 27, 28]:

$$N = \frac{e^2 E_S^2}{4\pi^2\hbar^2 c} \int dV \int_{-\infty}^{+\infty} dt \varepsilon\eta \coth\frac{\pi\eta}{\varepsilon} \exp\left(-\frac{\pi}{\varepsilon}\right) \tag{4}$$

with the approximation that the volume and time are much larger than the Compton wavelength, $\lambda\!\!\!^{-}_C \equiv \hbar/m_e c$, and corresponding time $\lambda\!\!\!^{-}_C/c$, respectively, where $\varepsilon = \mathcal{E}/E_S$ $\eta = \mathcal{H}/E_S$, $\mathcal{E} = \sqrt{(\mathcal{F}^2 + \mathcal{G}^2)^{1/2} + \mathcal{F}}$ and $\mathcal{H} = \sqrt{(\mathcal{F}^2 + \mathcal{G}^2)^{1/2} - \mathcal{F}}$ are invariant electric and magnetic fields, respectively, $\mathcal{F} =$

$(\mathbf{E}^2 - \mathbf{B}^2)/2$ and $\mathcal{G} = \mathbf{E} \cdot \mathbf{B}/2$ are Poincare invariants of the electromagnetic field with $(\mathbf{E}, \mathbf{B})$ being the electric and magnetic fields, respectively.

In the case of a spherically symmetric micro-bubble implosion only the electrostatic field is present. So that $\mathcal{E} = \mathbf{E}$ and $\mathcal{H} = 0$ resulting in $\varepsilon = \mathcal{E}/E_S$ and $\eta = 0$. Equation 4 becomes:

$$N = \frac{e^2 E_S^2}{4\pi^2 \hbar^2 c} \int_{-\infty}^{+\infty} dt \int dr 4\pi r^2 \frac{\varepsilon^2}{\pi} \exp\left(-\frac{\pi}{\varepsilon}\right) \tag{5}$$

assuming spherical symmetry. The electric field around the core at maximum compression is given by a 1D model as [21]:

$$E_f(r) = \frac{eN_{e0}}{2R_0 r_{min}} \left(\frac{r_{min}}{r} - \frac{r_{min}^2}{r^2}\right), r \geq r_{min} \tag{6}$$

so that $\varepsilon(r) = E_f(r)/E_S$. Eq. 5 can be simplified and integrated assuming that the main contribution to the pair creation comes from the maximum compression of the bubble:

$$N \approx \frac{e^2 E_S^2}{\pi^2 \hbar^2 c} \Delta t \int_{r_{min}}^{\mathbf{R_0}} dr \varepsilon(r)^2 r^2 \exp\left(-\frac{\pi}{\varepsilon(r)}\right) \tag{7}$$

where Δt is the duration of the maximum compression. Equation 7 can be re-expressed as:

$$N \approx \frac{r_{min}^3 c \Delta t}{\pi^2 \lambda\!\!\!^{-4}_C} \int_1^{\mathbf{R_0/r_{min}}} dr' \varepsilon(r')^2 r'^2 \exp\left(-\frac{\pi}{\varepsilon(r')}\right) \tag{8}$$

where $r' = r/r_{min}$ and

$$\varepsilon(r') = \frac{N_{e0}}{2} \frac{r_e \lambda\!\!\!^{-}_C}{R_0 r_{min}} \left(\frac{1}{r'} - \frac{1}{r'^2}\right), r' \geq 1 \tag{9}$$

where r_e is the classical electron radius.

We numerically integrated Eq. 8 and in Fig. 3 plot the number of pairs created by varying the initial (a) average electron density, $n/\tilde{n}_{e0}$, and (b) radius of the bubble, R/R_0, using the typical parameters of the micro-bubble implosion from the previous section keeping the other parameters fixed for maximum compression duration of 0.01 fs, which was taken from the stagnation time of 10 as observed in simulations[21]. **Theoretically the maximum compression duration can be calculated from the time evolution of the innermost**

spherical shell at the time of maximum compression. The equation of motion of a test proton of mass m_p on the innermost shell is given by:

$$m_p \ddot{r} = \frac{\frac{1}{2} N_a e^2}{r^2} \tag{10}$$

where the factor of $1/2$ comes from the fact that the test proton is on the same radius of the shell with [20] $N_a = 4\pi(R_0/d_0)^2$ where $d_0 = n_{i0}^{-1/3}$ is the characteristic interatomic distance on the initial bubble surface. Taking the characteristic size at the maximum compression to be $r \to r_{min}$ the resulting characteristic time of the explosion is:

$$t_0 = \sqrt{\frac{27}{2} \frac{m_p n_{i0}^{4/3}}{\pi R_0^2 \bar{n}_{e0}^3 e^2}} = \sqrt{\frac{27}{2\pi} \left(\frac{m_p}{m_e}\right) \left(\frac{n_{i0}^{4/3}}{\bar{n}_{e0}^3}\right) \frac{1}{R_0^2 r_e c^2}}. \tag{11}$$

Using typical values of $n_{i0} = 5 \times 10^{22} \mathbf{cm}^{-3}$, $\tilde{n}_{e0} = 5 \times 10^{21} \mathbf{cm}^{-3}$, and $R_0 = 2\mu\mathbf{m}$ the typical timescale becomes $t_0 \approx 0.1$ fs $= 100$ as, which is also plotted in Fig. 3 as the maximum compression duration.

From the figures it can be seen that **for both compression times** pairs start to be created around $n/\tilde{n}_{e0} \approx 9$ corresponding to an initial average electron density of $\sim 4.5 \times 10^{22}$ cm^{-3} in Fig. 3(a) and $R/R_0 \approx 8$ corresponding to an initial radius of $\sim 16\mu$m in Fig. 3(b). Both values from Fig. 3(a) and (b) correspond to maximum electrostatic fields of $E_{max}/E_S \sim 0.1$ as seen in Fig. 2. As stated in the previous section it may be easier to achieve pair creation by increasing $\tilde{n}_{e0}$ rather than R_0. **With $R/R_0 \approx 8$ a laser spot eight times larger and based on the scaling of intensity [21] with R_0 an intensity 8^4 times higher resulting in $\approx 2.6 \times 10^5$ times the amount of laser energy would be necessary to cover the bubble whereas $n/\tilde{n}_{e0} \approx 9$ would require the same amount of laser energy, but with a modification of the target.**

For a clearer understanding of the relationship between $\tilde{n}_{e0}$ and R_0 a contour plot showing the number of pairs created versus both parameters is shown in Fig. 4 assuming a maximum compression time

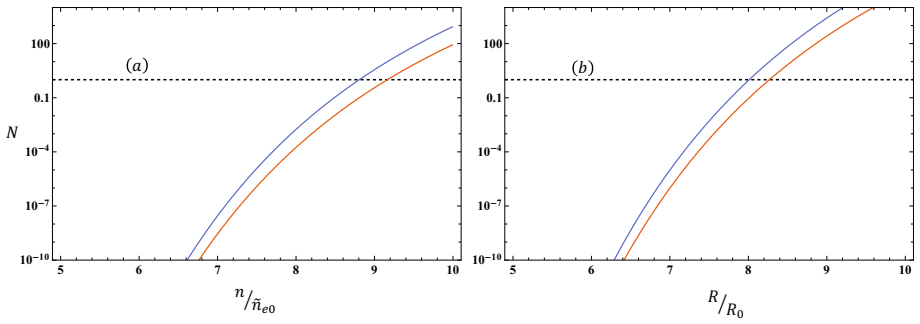

Figure 3: Number of pairs created in a micro-bubble implosion varying the initial (a) average electron density, $n/\tilde{n}_{e0}$, and (b) radius of the bubble, R/R_0, keeping the other typical parameters of $n_{i0} = 5 \times 10^{22}\text{cm}^{-3}$, $\tilde{n}_{e0} = 5 \times 10^{21}\text{cm}^{-3}$, and $R_0 = 2\mu$m fixed for a maximum compression duration of $\Delta t = 0.01$ fs **(red line) and** $\Delta t = 0.1$ **fs (blue line)**. The vertical dotted lines in (a) and (b) refer to $n/\tilde{n}_{e0} = 1$ and $R/R_0 = 1$, respectively. The dashed lines refer to $N = 1$.

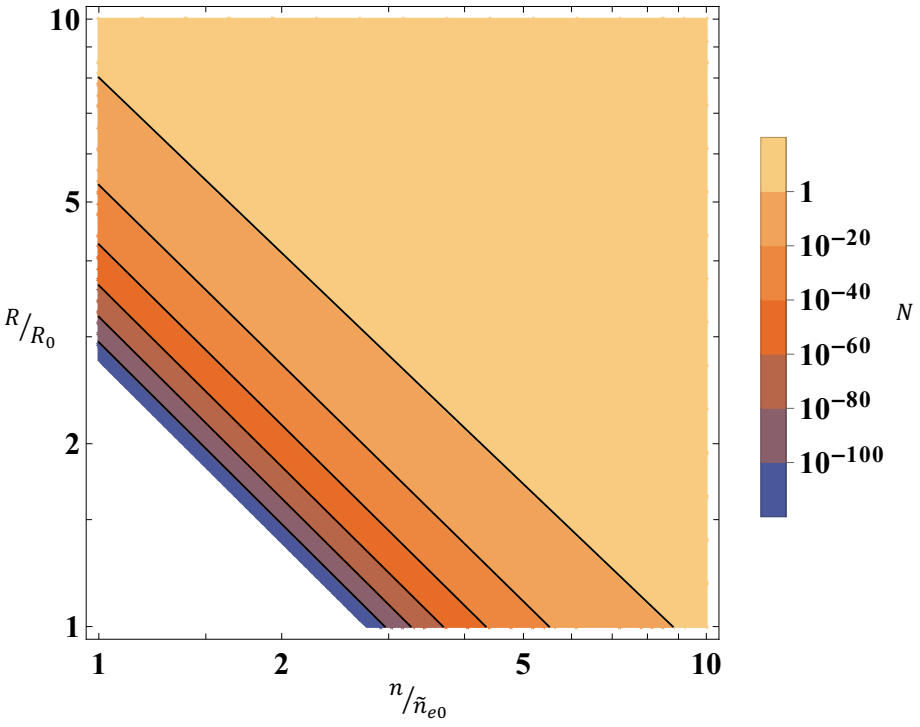

Figure 4: Number of pairs, N, created in a micro-bubble implosion versus the initial average electron density, $n/\tilde{n}_{e0}$, and radius of the bubble, R/R_0, for a maximum compression duration of $\Delta t = 0.1$ fs.

of $\Delta t = 0.1$ fs. As can be seen in the figure isocontour lines occur along $n \times R =$constant. This is a consequence of the fact that the number of pairs strongly depends on the argument in the exponential function in Eq. 8 which is $\varepsilon(r')$. This in turn has a pre-factor which depends on $N_{e0}/R_0 r_{min} \propto (R_0 \tilde{n}_{e0})^2$. This will be a very important criterion in future target design.

It should be noted here that increasing $\tilde{n}_{e0}$ by coating the target surface with a high-Z material could lead to direct production of electron-positron pairs from Bethe-Heitler (BH) or Trident processes due to the high intensity laser target interaction [29]. **In the next section we roughly estimate the contributions.** However, we consider this to be beyond the scope of the current paper and leave it for further consideration.

4. Pair creation in the Micro-bubble Implosion from Background or Externally Injected Gamma-rays and Electrons

In the previous section we examined the possibility of electron-positron pair creation from the vacuum due to the electrostatic field generated by the micro-bubble implosion. In this section we consider under what conditions (1) background high energy electrons and photons inherent in the environment of the micro-bubble implosion or (2) external source of gamma-rays and electrons traveling through these fields could induce pair creation even when the electrostatic field itself doesn't create pairs. The quantum electrodynamic (QED) gauge invariant parameters, χ_e and χ_γ, characterize the probability of gamma-ray emission by an electron and electron-positron pair creation by a gamma-ray, respectively, interacting with electromagnetic fields, which are expressed in terms of electric and magnetic fields as (see for example [30] and references cited therein):

$$\chi_e = \frac{1}{E_S m_e c}\sqrt{(m_e c \gamma_e \mathbf{E} + \mathbf{p} \times \mathbf{B})^2 - (\mathbf{p} \cdot \mathbf{B})^2} \tag{12}$$

$$\chi_\gamma = \frac{\hbar}{E_S m_e c}\sqrt{(\frac{\omega_\gamma}{c}\mathbf{E} + \mathbf{k}_\gamma \times \mathbf{B})^2 - (\mathbf{k}_\gamma \cdot \mathbf{E})^2} \tag{13}$$

where (γ_e, $\mathbf{p}$) are the relativistic gamma factor and momentum of the electron, respectively, (ω_γ, $\mathbf{k}_\gamma$) are the frequency and wave vector of the photon, respectively, and when $\chi_e, \chi_\gamma > 1$, the conditions are optimal for pair creation. For $\mathbf{B} = 0$ the parameters become:

$$\chi_e \approx \gamma_e \frac{E}{E_S} \tag{14}$$

$$\chi_\gamma \approx \frac{\hbar\omega_\gamma}{m_e c^2} \frac{E}{E_S} \tag{15}$$

Eqs. 14 and 15 indicate optimal conditions, when $\boldsymbol{\gamma_e, \frac{\hbar\omega_\gamma}{m_e c^2} > \frac{E_S}{E}}$. So for the typical parameters of [20] $E_{max}/E_S \approx 1.4 \times 10^{-3}$ this implies pair creation from background electrons or photons when $E_e, E_\gamma > 365$ MeV where E_e and E_γ refer the electron and photon energy, respectively.

An additional factor given the small size of the micro-bubble region is the formation length [31, 32]. For pair creation from a photon the formation length, l_f^{pair} is given by [32]:

$$l_f^{pair} = \frac{2\gamma_p^2 c}{\omega'} \tag{16}$$

where $\gamma_p \equiv \hbar\omega_\gamma / m_e c^2$ and $\omega' = \omega_\gamma / \eta_+ \eta_-$ with $\eta_\pm \equiv E_{e^\pm}/\hbar\omega_\gamma$ and $E_{e^\pm}$ being the energy of the created electron or positron. Using the values for the pair creation of $E_\gamma > 365$ MeV implies $\gamma_p > 714$ and assuming that the electrons and positrons are created with energies of $E_{e^\pm} \approx \hbar\omega_\gamma/2$, which are predominant for $\chi_\gamma < 8$ [33], resulting in $\omega' = 4\omega_\gamma$, then $l_f^{pair} > 0.55$nm. This is more than an order of magnitude smaller than the minimum radius $r_{min} = 8.14$nm at the maximum compression calculated from the typical parameters of [20]. So pairs created from high energy photons are possible in the micro-bubble.

The formation length for photons from high energy electrons, l_f, is [32]:

$$l_f = \frac{2\gamma^2 c}{\omega^*} \tag{17}$$

where

$$\omega^* = \omega \frac{E_T}{E_T - \hbar\omega}, \tag{18}$$

$E_T = m_e c^2 + E_e$ is the total energy of the electron, γ is the relativistic gamma factor of the electron, ω is the frequency of the emitted photon assuming the photon emission angle is $\theta \simeq 1/\gamma$, the electron scattering angle is $\psi \simeq 0$, and sufficiently high photon energies $\hbar\omega \gtrsim \gamma\hbar\omega_{pe}$ where $\omega_{pe} = \sqrt{4\pi e^2 nZ/m_e}$ is the the plasma frequency with Z being the atomic number of the material and n being the number density. In the case of the micro-bubble implosion the plasma frequency is further reduced due to the relativistic nature of the background electrons to $\omega_{pe} = \sqrt{4\pi e^2 nZ/\gamma_{th} m_e}$ where γ_{th} would be the relativistic gamma factor of the thermal background electrons. Even when this is not taken into account and assuming the electron density could reach the maximum compression ion density, n_{max}, of the core [20]:

$$\frac{n_{max}}{n_{i0}} = \left(\frac{N_{e0}}{6^{7/2}\pi}\right)^{2/3}, \tag{19}$$

which is $n_{max} = 2.16 \times 10^5 n_{i0} \approx 10^{28}\text{cm}^{-3}$, this results in $\hbar\omega_{pe} \approx 4$ keV when multiplied by γ for a 365 MeV electron becomes $\gamma\hbar\omega_{pe} \approx 2.8$ MeV. So for 365 MeV photons $\hbar\omega \gtrsim \gamma\hbar\omega_{pe}$ is satisfied. Therefore, using Eq. 17 is justified. Assuming $E_e = 365$ MeV and that the emitted photon has the same energy we get $l_f \approx 0.55$ nm. This is far below the scale size of the compressed core meaning that pairs could be created.

The temperature of the hot background electrons from the pondermotive scaling is given by [21] $T_{hot} \simeq 44\left(I_{L22}\lambda_{L\mu}^2\right)$ **where** I_{L22} **is the laser intensity in units of** $10^{22}\mathbf{W/cm^2}$ **and** $\lambda_{L\mu}$ **is the laser wavelength in units of** μ**m. The required temperature depends on** $\Lambda \equiv R_0/\Lambda_{Di}$**, which is the ratio of the initial bubble radius,** R_0 **to the ion Debye length,** $\lambda_{Di} = \sqrt{T_{hot}/4\pi n_{i0} e^2}$ **[21]. For** $\Lambda = 2.5$ **the temperature is** ~ 400 **MeV with** $I = 1.75 \times 10^{24}$ **W/cm**^{2} **and** $\lambda = 1\mu$**m. For** $\Lambda = 6$ **the temperature is** ~ 98 **MeV with** $I = 5 \times 10^{22}$ **W/cm**^{2} **and** $\lambda = 1\mu$**m. From this we can see that the hot background electrons in the case of** $\Lambda = 2.5$ **could generate pairs during the maximum compression time of the core, which is estimated as 100 as above. In the case where the pairs are generated directly from the vacuum such short duration flashes**

of pairs would also be expected.

If an external source of gamma-rays and electrons having energies greater than 365 MeV are injected into the micro-bubble region they could induce the creation of pairs. However, at much higher photon or electron energies when their respective formation lengths become larger than the scale size of the bubble, $\left(l_f^{pair}, l_f\right) \gtrapprox 2r_{min}$, the creation of pairs is suppressed. Additionally, lower energy electrons could be injected into the micro-bubble region to diagnose the imploded core due to their scattering by the extremely strong electrostatic field there.

In principle the formation length depends on the energy of emitted particle (see [34]), but for the highest energy particles the above estimates should be sufficient.

Several types of high power gamma-ray sources have been proposed [18, 19, 35]. Given that the maximum implosion core size and timescales are on the order of 10's nm and 10's to 100's of attoseconds, respectively, the required gamma-ray beam luminosity would be approximately $\mathcal{L} \sim 1/(10^{-6}\mathbf{cm})^2/(10^{-16\sim17}\mathbf{s}) = 10^{28\sim29}/\mathbf{cm}^2\mathbf{s}$ assuming at least one photon is in the target area. By colliding high-energy electron beams with strong laser fields gamma-ray beams with densities for energies of the order of $n_\gamma \sim 10^{18}\mathbf{cm}^{-3}$ for multi-GeV [18] and $n_\gamma \sim 10^{20}\mathbf{cm}^{-3}$ for hundreds of MeV [19] have been shown, respectively. The resulting luminosities are $\mathcal{L} \sim n_\gamma c = 3 \times 10^{28}/\mathbf{cm}^2\mathbf{s}$ for multi-GeV photons and $\mathcal{L} \sim n_\gamma c = 3 \times 10^{30}/\mathbf{cm}^2\mathbf{s}$ for hundreds of MeV photons, which are both of the order of the required luminosity.

Since the typical densities of laser wakefield accelerated electron beams are of the order of the above gamma-ray beams, the required luminosity can be achieved. One concern would be whether the electromagnetic fields produced by the beams would disturb the imploded core fields. Assuming that the electron beam is a uniform density cylinder the radial electric field of the beam would approximately be with respect to the Schwinger field $E_r/E_S \sim \pi\gamma n_e r_b r_e \lambda\!\!\!^{-}_C$ where π, γ, n_e

and r_b are the relativistic gamma factor, electron beam density, and electron beam radius, respectively. Taking that the high energy electron beam is generated via laser wakefield acceleration the typical beam parameters would be [36] $\gamma = 10^3$ (500 MeV), $n_e \sim 10^{18}$ cm^{-3}, $r_b \sim 5 \times 10^{-4}$ cm giving $E_r/E_S \sim 1.7 \times 10^{-5}$ at the electron beam edge where the field is maximal. This is roughly two orders of magnitude below the maximum field attained by the micro-bubble implosion of $E_{max}/E_S = 1.4 \times 10^{-3}$ for typical parameters. In addition, since the imploded core field is positive, the electron beam should be attracted to and be able to penetrate the bubble field.

In addition to the pair creation mechanism we have discussed above there will be two other competing processes: Bethe-Heitler [37] and Trident [37, 38, 39] (see perspectives article [40] for more discussions of this in relativistic plasmas). For thin targets, for example less than 30 microns of solid gold, the Trident process is expected to dominate over the Bethe-Heitler process [41]. Since we do not consider thick targets of high Z material we use the cross section for Trident production to estimate the number of positrons produced in the target assuming that the energy loss of electrons traveling through the target is minimal. The cross section is $\sim Z^2\alpha^2 r_e^2$ (see [42] and cited references). We assume that the electrons accelerated from the surface have a density of $n_e = 5 \times 10^{21-22}$ cm^{-3} with a beam size comparable to the laser spot size of $R_0 = 2\mu$m with velocities nearly the speed of light and a duration comparable to the laser pulse duration, which we take to be 30 fs, and travel thru a target of 10μ thickness having an ion density of 5×10^{22} cm^{-3} with an atomic number of $Z = 1$. The number of pairs created via the Trident process is $\sim 40 - 400$ in each direction. This number is small. In addition, since the laser intensities we are considering are where a large portion of the laser energy could be converted to high energy gamma-rays [43], the Breit-Wheeler process could generate a large number of pairs.

However, if the pre-plasma density scale length in front of the target is small the conversion is smaller [43]. Thus having an extremely high contrast is advantageous for minimizing this effect. Further detailed investigation requires investigation with PIC codes including these processes [44, 45]. However, due to the large ratio between the initial bubble size and the compressed core extremely large computational resources for the required resolution would be necessary in addition to properly modeling the collisions of photons for the Breit-Wheeler pair production process.

5. Discussion and Conclusions

We have investigated the possibility of electron-positron pair creation from the vacuum due to micro-bubble implosions. We have found that the typical parameters found in [20] for a micro-bubble implosion will not lead to electrostatic fields generated by the imploded core sufficiently high enough for pair generation from the vacuum. However, by either increasing the initial bubble radius from 2μm by a factor ≈ 8 or average electron density in the bubble from 5×10^{21} cm^{-3} by a factor ≈ 9 electrostatic fields of sufficient amplitude to generate pairs from the vacuum could be possible. The simplest way to do this would be to increase the average initial background electron density by coating the initial hydrogen solid with a higher Z material such as plastic (CH) [21] or Gold. **As a result, a pair creation from vacuum could be possible with a $\sim 200 - 300$ PW laser of energy $\sim 2 - 3$ kJ.**

Although a detailed study is required, a possible experimental configuration for the target could involve already experimentally used cryogenic solid hydrogen jets [46] or ribbons [47] with hollow carbon spheres (HCS) [48] embedded within them. The jets and ribbons have thicknesses on the order of 10's of μm [46, 47] and the HCS have sizes ranging from nm to mm [48]. The determination of the optimum target and laser parameters where other QED processes,

such as Trident, Bethe-Heitler and Breit-Wheeler pair creation are sufficiently minimized will require PIC simulations including these processes [44, 45]. However, this will require huge computational resources along with determining the proper techniques to model photon collisions for the Breit-Wheeler pair production.

In addition we have found that even with electrostatic fields below the threshold for pair production background or externally injected electrons or photons of sufficiently high energy, greater than 365 MeV, could induce pair creation. This makes micro-bubble implosions interesting targets for studying the pair creation process.

6. Acknowledgements

M. Murakami was supported by the Japan Society for the Promotion of Science (JSPS). A. V. Arefiev was supported by U.S. Air Force Project AFOSR No. FA9550-17-1-0382. Y. Nakamiya was supported by the Extreme Light Infrastructure Nuclear Physics (ELI-NP) Phase II, a project co-financed by the Romanian Government and the European Union through the European Regional Development Fund-the Competitiveness Operational Programme (1/07.07.2016, COP, ID 1334). **S. S. Bulanov acknowledges the support from the U.S. DOE Office of Science Offices of HEP and FES (through LaserNetUS), under Contract No. DE-AC02-05CH11231.** S. V. Bulanov was supported by the project High Field Initiative (CZ.02.1.01/0.0/0.0/15_003/0000449) from the European Regional Development Fund.

References

[1] F. Sauter, Über das verhalten eines elektrons im homogenen elektrischen feld nach der relativistischen theorie diracs, Zeitschrift für Physik 69 (11) (1931) 742–764. doi:10.1007/BF01339461.
URL https://doi.org/10.1007/BF01339461

[2] W. Heisenberg, H. Euler, Folgerungen aus der diracschen theorie des positrons, Zeitschrift für Physik 98 (11) (1936) 714–732. doi:10.1007/BF01343663.
URL https://doi.org/10.1007/BF01343663

[3] J. Schwinger, On gauge invariance and vacuum polarization, Phys. Rev. 82 (1951) 664–679. doi:10.1103/PhysRev.82.664.
URL https://link.aps.org/doi/10.1103/PhysRev.82.664

[4] D. Strickland, G. Mourou, Compression of amplified chirped optical pulses, Optics Communications 55 (6) (1985) 447 – 449. doi:https://doi.org/10.1016/0030-4018(85)90151-8.
URL http://www.sciencedirect.com/science/article/pii/0030401885901518

[5] A. S. Pirozhkov, Y. Fukuda, M. Nishiuchi, H. Kiriyama, A. Sagisaka, K. Ogura, M. Mori, M. Kishimoto, H. Sakaki, N. P. Dover, K. Kondo, N. Nakanii, K. Huang, M. Kanasaki, K. Kondo, M. Kando, Approaching the diffraction-limited, bandwidth-limited petawatt, Opt. Express 25 (17) (2017) 20486–20501. doi:10.1364/OE.25.020486.
URL http://www.opticsexpress.org/abstract.cfm?URI=oe-25-17-20486

[6] H. Kiriyama, A. S. Pirozhkov, M. Nishiuchi, Y. Fukuda, K. Ogura, A. Sagisaka, Y. Miyasaka, M. Mori, H. Sakaki, N. P. Dover, K. Kondo, J. K. Koga, T. Z. Esirkepov, M. Kando, K. Kondo, High-contrast high-intensity repetitive petawatt laser, Opt. Lett. 43 (11) (2018) 2595–2598. doi:10.1364/OL.43.002595.
URL http://ol.osa.org/abstract.cfm?URI=ol-43-11-2595

[7] V. Yanovsky, V. Chvykov, G. Kalinchenko, P. Rousseau, T. Planchon, T. Matsuoka, A. Maksimchuk, J. Nees, G. Cheriaux, G. Mourou, K. Krushelnick, Ultra-high intensity- 300-TW laser at 0.1 Hz repetition rate., Opt. Express 16 (3) (2008) 2109–2114. doi:10.1364/OE.16.002109.

URL http://www.opticsexpress.org/abstract.cfm?URI=oe-16-3-2109

[8] J. W. Yoon, C. Jeon, J. Shin, S. K. Lee, H. W. Lee, I. W. Choi, H. T. Kim, J. H. Sung, C. H. Nam, Achieving the laser intensity of 5.5×10^{22} W/cm^2 with a wavefront-corrected multi-PW laser, Opt. Express 27 (15) (2019) 20412–20420. doi:10.1364/OE.27.020412.
URL http://www.opticsexpress.org/abstract.cfm?URI=oe-27-15-20412

[9] S. Gales, K. A. Tanaka, D. L. Balabanski, F. Negoita, D. Stutman, O. Tesileanu, C. A. Ur, D. Ursescu, I. Andrei, S. Ataman, M. O. Cernaianu, L. D'Alessi, I. Dancus, B. Diaconescu, N. Djourelov, D. Filipescu, P. Ghenuche, D. G. Ghita, C. Matei, K. Seto, M. Zeng, N. V. Zamfir, The extreme light infrastructure—nuclear physics (ELI-NP) facility: new horizons in physics with 10 PW ultra-intense lasers and 20 MeV brilliant gamma beams, Reports on Progress in Physics 81 (9) (2018) 094301.
URL http://stacks.iop.org/0034-4885/81/i=9/a=094301

[10] B. L. Garrec, S. Sebban, D. Margarone, M. Precek, S. Weber, O. Klimo, G. Korn, B. Rus, ELI-beamlines: extreme light infrastructure science and technology with ultra-intense lasers, in: Proc.SPIE, Vol. 8962, 2014, pp. 8962 – 8962 – 8.

[11] D. N. Papadopoulos, P. Ramirez, K. Genevrier, L. Ranc, N. Lebas, A. Pellegrina, C. L. Blanc, P. Monot, L. Martin, J. P. Zou, F. Mathieu, P. Audebert, P. Georges, F. Druon, High-contrast 10 fs OPCPA-based front end for multi-PW laser chains, Opt. Lett. 42 (18) (2017) 3530–3533. doi:10.1364/OL.42.003530.
URL http://ol.osa.org/abstract.cfm?URI=ol-42-18-3530

[12] B. Shen, Z. Bu, J. Xu, T. Xu, L. Ji, R. Li, Z. Xu, Exploring vacuum birefringence based on a 100 PW laser and an x-ray free electron laser

beam, Plasma Physics and Controlled Fusion 60 (4) (2018) 044002.
URL http://stacks.iop.org/0741-3335/60/i=4/a=044002

[13] B. Shao, Y. Li, Y. Peng, P. Wang, J. Qian, Y. Leng, R. Li, Broad-bandwidth high-temporal-contrast carrier-envelope-phase-stabilized laser seed for 100pw lasers, Opt. Lett. 45 (8) (2020) 2215–2218. doi:10.1364/OL.390110.
URL http://ol.osa.org/abstract.cfm?URI=ol-45-8-2215

[14] C. N. Danson, C. Haefner, J. Bromage, T. Butcher, J.-C. F. Chanteloup, E. A. Chowdhury, A. Galvanauskas, L. A. Gizzi, J. Hein, D. I. Hillier, et al., Petawatt and exawatt class lasers worldwide, High Power Laser Science and Engineering 7 (2019) e54. doi:10.1017/hpl.2019.36.

[15] S. S. Bulanov, V. D. Mur, N. B. Narozhny, J. Nees, V. S. Popov, Multiple colliding electromagnetic pulses: A way to lower the threshold of e^+e^- pair production from vacuum, Phys. Rev. Lett. 104 (2010) 220404. doi:10.1103/PhysRevLett.104.220404.
URL https://link.aps.org/doi/10.1103/PhysRevLett.104.220404

[16] S. S. Bulanov, T. Z. Esirkepov, A. G. R. Thomas, J. K. Koga, S. V. Bulanov, Schwinger limit attainability with extreme power lasers, Phys. Rev. Lett. 105 (2010) 220407. doi:10.1103/PhysRevLett.105.220407.
URL https://link.aps.org/doi/10.1103/PhysRevLett.105.220407

[17] A. Gonoskov, I. Gonoskov, C. Harvey, A. Ilderton, A. Kim, M. Marklund, G. Mourou, A. Sergeev, Probing nonperturbative QED with optimally focused laser pulses, Phys. Rev. Lett. 111 (2013) 060404. doi:10.1103/PhysRevLett.111.060404.
URL https://link.aps.org/doi/10.1103/PhysRevLett.111.060404

[18] J. Magnusson, A. Gonoskov, M. Marklund, T. Z. Esirkepov, J. K. Koga, K. Kondo, M. Kando, S. V. Bulanov, G. Korn, S. S. Bulanov, Laser-particle collider for Multi-GeV photon production, Phys. Rev. Lett. 122 (2019)

254801. doi:10.1103/PhysRevLett.122.254801.
URL https://link.aps.org/doi/10.1103/PhysRevLett.122.254801

[19] J. Magnusson, A. Gonoskov, M. Marklund, T. Z. Esirkepov, J. K. Koga, K. Kondo, M. Kando, S. V. Bulanov, G. Korn, C. G. R. Geddes, C. B. Schroeder, E. Esarey, S. S. Bulanov, Multiple colliding laser pulses as a basis for studying high-field high-energy physics, Phys. Rev. A 100 (2019) 063404. doi:10.1103/PhysRevA.100.063404.
URL https://link.aps.org/doi/10.1103/PhysRevA.100.063404

[20] M. Murakami, A. Arefiev, M. A. Zosa, Generation of ultrahigh field by micro-bubble implosion, Scientific Reports 8 (1) (2018) 7537. doi:10.1038/s41598-018-25594-3.
URL https://doi.org/10.1038/s41598-018-25594-3

[21] M. Murakami, A. Arefiev, M. A. Zosa, J. K. Koga, Y. Nakamiya, Relativistic proton emission from ultrahigh-energy-density nanosphere generated by microbubble implosion, Physics of Plasmas 26 (4) (2019) 043112. doi:10.1063/1.5093043.
URL https://doi.org/10.1063/1.5093043

[22] J. K. Koga, M. Murakami, A. V. Arefiev, Y. Nakamiya, Probing and possible application of the QED vacuum with micro-bubble implosions induced by ultra-intense laser pulses, Matter and Radiation at Extremes 4 (3) (2019) 034401. doi:10.1063/1.5086933.
URL https://doi.org/10.1063/1.5086933

[23] S. C. Wilks, A. B. Langdon, T. E. Cowan, M. Roth, M. Singh, S. Hatchett, M. H. Key, D. Pennington, A. MacKinnon, R. A. Snavely, Energetic proton generation in ultra-intense laser–solid interactions, Physics of Plasmas 8 (2) (2001) 542–549. doi:10.1063/1.1333697.
URL https://doi.org/10.1063/1.1333697

[24] A. Yogo, K. Mima, N. Iwata, S. Tosaki, A. Morace, Y. Arikawa, S. Fujioka,

T. Johzaki, Y. Sentoku, H. Nishimura, A. Sagisaka, K. Matsuo, N. Kamitsukasa, S. Kojima, H. Nagatomo, M. Nakai, H. Shiraga, M. Murakami, S. Tokita, J. Kawanaka, N. Miyanaga, K. Yamanoi, T. Norimatsu, H. Sakagami, S. V. Bulanov, K. Kondo, H. Azechi, Boosting laser-ion acceleration with multi-picosecond pulses, Scientific Reports 7 (1) (2017) 42451. doi:10.1038/srep42451.
URL https://doi.org/10.1038/srep42451

[25] D. Mariscal, T. Ma, S. C. Wilks, A. J. Kemp, G. J. Williams, P. Michel, H. Chen, P. K. Patel, B. A. Remington, M. Bowers, L. Pelz, M. R. Hermann, W. Hsing, D. Martinez, R. Sigurdsson, M. Prantil, A. Conder, J. Lawson, M. Hamamoto, P. Di Nicola, C. Widmayer, D. Homoelle, R. Lowe-Webb, S. Herriot, W. Williams, D. Alessi, D. Kalantar, R. Zacharias, C. Haefner, N. Thompson, T. Zobrist, D. Lord, N. Hash, A. Pak, N. Lemos, M. Tabak, C. McGuffey, J. Kim, F. N. Beg, M. S. Wei, P. Norreys, A. Morace, N. Iwata, Y. Sentoku, D. Neely, G. G. Scott, K. Flippo, First demonstration of arc-accelerated proton beams at the national ignition facility, Physics of Plasmas 26 (4) (2019) 043110. arXiv:https://doi.org/10.1063/1.5085787, doi:10.1063/1.5085787.
URL https://doi.org/10.1063/1.5085787

[26] N. Narozhny, S. Bulanov, V. Mur, V. Popov, e+e-pair production by a focused laser pulse in vacuum, Physics Letters A 330 (1) (2004) 1 – 6. doi:https://doi.org/10.1016/j.physleta.2004.07.013.
URL http://www.sciencedirect.com/science/article/pii/S0375960104009971

[27] N. B. Narozhny, S. S. Bulanov, V. D. Mur, V. S. Popov, On e+e- pair production by colliding electromagnetic pulses, Journal of Experimental and Theoretical Physics Letters 80 (6) (2004) 382–385. doi:10.1134/1.1830652.
URL https://doi.org/10.1134/1.1830652

[28] S. S. Bulanov, N. B. Narozhny, V. D. Mur, V. S. Popov, Electron-positron pair production by electromagnetic pulses, Journal of Experimental and Theoretical Physics 102 (1) (2006) 9–23. doi:10.1134/S106377610601002X.
URL https://doi.org/10.1134/S106377610601002X

[29] H. Chen, S. C. Wilks, J. D. Bonlie, E. P. Liang, J. Myatt, D. F. Price, D. D. Meyerhofer, P. Beiersdorfer, Relativistic positron creation using ultraintense short pulse lasers, Phys. Rev. Lett. 102 (2009) 105001. doi:10.1103/PhysRevLett.102.105001.
URL https://link.aps.org/doi/10.1103/PhysRevLett.102.105001

[30] S. Bulanov, T. Esirkepov, Y. Hayashi, M. Kando, H. Kiriyama, J. Koga, K. Kondo, H. Kotaki, A. Pirozhkov, S. Bulanov, A. Zhidkov, P. Chen, D. Neely, Y. Kato, N. Narozhny, G. Korn, On the design of experiments for the study of extreme field limits in the interaction of laser with ultrarelativistic electron beam, Nuclear Instruments and Methods in Physics Research Section A: Accelerators, Spectrometers, Detectors and Associated Equipment 660 (1) (2011) 31 – 42. doi:https://doi.org/10.1016/j.nima.2011.09.029.
URL http://www.sciencedirect.com/science/article/pii/S0168900211017840

[31] V. Baier, V. Katkov, Concept of formation length in radiation theory, Physics Reports 409 (5) (2005) 261 – 359. doi:https://doi.org/10.1016/j.physrep.2004.11.003.
URL http://www.sciencedirect.com/science/article/pii/S0370157304005083

[32] U. I. Uggerhøj, The interaction of relativistic particles with strong crystalline fields, Rev. Mod. Phys. 77 (2005) 1131–1171. doi:10.1103/RevModPhys.77.1131.
URL https://link.aps.org/doi/10.1103/RevModPhys.77.1131

[33] S. S. Bulanov, C. B. Schroeder, E. Esarey, W. P. Leemans, Electromagnetic cascade in high-energy electron, positron, and photon interactions with intense laser pulses, Phys. Rev. A 87 (2013) 062110. doi:10.1103/PhysRevA.87.062110.
URL https://link.aps.org/doi/10.1103/PhysRevA.87.062110

[34] T. G. Blackburn, D. Seipt, S. S. Bulanov, M. Marklund, Radiation beaming in the quantum regime, Phys. Rev. A 101 (2020) 012505. doi:10.1103/PhysRevA.101.012505.
URL https://link.aps.org/doi/10.1103/PhysRevA.101.012505

[35] T. Wang, X. Ribeyre, Z. Gong, O. Jansen, E. d'Humières, D. Stutman, T. Toncian, A. Arefiev, Power scaling for collimated γ-ray beams generated by structured laser-irradiated targets and its application to two-photon pair production, Phys. Rev. Applied 13 (2020) 054024. doi:10.1103/PhysRevApplied.13.054024.
URL https://link.aps.org/doi/10.1103/PhysRevApplied.13.054024

[36] E. Esarey, C. B. Schroeder, W. P. Leemans, Physics of laser-driven plasma-based electron accelerators, Rev. Mod. Phys. 81 (2009) 1229–1285. doi:10.1103/RevModPhys.81.1229.
URL https://link.aps.org/doi/10.1103/RevModPhys.81.1229

[37] W. Heitler, The Quantum Theory of Radiation, Dover Books on Physics, Dover Publications, 1984.
URL https://books.google.co.jp/books?id=L7w7UpecbKYC

[38] D. A. Gryaznykh, Y. Z. Kandiev, V. A. Lykov, Estimates of electron-positron pair production in the interaction of high-power laser radiation with high-z targets, Journal of Experimental and Theoretical Physics Letters 67 (4) (1998) 257–262. doi:10.1134/1.567660.
URL https://doi.org/10.1134/1.567660

[39] K. Nakashima, H. Takabe, Numerical study of pair creation by ultraintense lasers, Physics of Plasmas 9 (5) (2002) 1505–1512. arXiv:https://doi.

org/10.1063/1.1464145, doi:10.1063/1.1464145.
URL https://doi.org/10.1063/1.1464145

[40] P. Zhang, S. S. Bulanov, D. Seipt, A. V. Arefiev, A. G. R. Thomas, Relativistic plasma physics in supercritical fields, Physics of Plasmas 27 (5) (2020) 050601. arXiv:https://doi.org/10.1063/1.5144449, doi:10.1063/1.5144449.
URL https://doi.org/10.1063/1.5144449

[41] E. P. Liang, S. C. Wilks, M. Tabak, Pair production by ultraintense lasers, Phys. Rev. Lett. 81 (1998) 4887–4890. doi:10.1103/PhysRevLett.81.4887.
URL https://link.aps.org/doi/10.1103/PhysRevLett.81.4887

[42] X. Ribeyre, E. d'Humières, O. Jansen, S. Jequier, V. T. Tikhonchuk, M. Lobet, Pair creation in collision of γ-ray beams produced with high-intensity lasers, Phys. Rev. E 93 (2016) 013201. doi:10.1103/PhysRevE.93.013201.
URL https://link.aps.org/doi/10.1103/PhysRevE.93.013201

[43] T. Nakamura, J. K. Koga, T. Z. Esirkepov, M. Kando, G. Korn, S. V. Bulanov, High-power γ-ray flash generation in ultraintense laser-plasma interactions, Phys. Rev. Lett. 108 (2012) 195001. doi:10.1103/PhysRevLett.108.195001.
URL https://link.aps.org/doi/10.1103/PhysRevLett.108.195001

[44] T. D. Arber, K. Bennett, C. S. Brady, A. Lawrence-Douglas, M. G. Ramsay, N. J. Sircombe, P. Gillies, R. G. Evans, H. Schmitz, A. R. Bell, C. P. Ridgers, Contemporary particle-in-cell approach to laser-plasma modelling, Plasma Physics and Controlled Fusion 57 (11) (2015) 113001. doi:10.1088/0741-3335/57/11/113001.
URL https://doi.org/10.1088%2F0741-3335%2F57%2F11%2F113001

[45] B. Martinez, M. Lobet, R. Duclous, E. d'Humières, L. Gremillet, High-energy radiation and pair production by coulomb processes in particle-in-

cell simulations, Physics of Plasmas 26 (10) (2019) 103109. arXiv:https://doi.org/10.1063/1.5118339, doi:10.1063/1.5118339.
URL https://doi.org/10.1063/1.5118339

[46] J. Polz, A. P. L. Robinson, A. Kalinin, G. A. Becker, R. A. C. Fraga, M. Hellwing, M. Hornung, S. Keppler, A. Kessler, D. Klöpfel, H. Liebetrau, F. Schorcht, J. Hein, M. Zepf, R. E. Grisenti, M. C. Kaluza, Efficient laser-driven proton acceleration from a cryogenic solid hydrogen target, Scientific Reports 9 (1) (2019) 16534. doi:10.1038/s41598-019-52919-7.
URL https://doi.org/10.1038/s41598-019-52919-7

[47] D. Margarone, A. Velyhan, J. Dostal, J. Ullschmied, J. P. Perin, D. Chatain, S. Garcia, P. Bonnay, T. Pisarczyk, R. Dudzak, M. Rosinski, J. Krasa, L. Giuffrida, J. Prokupek, V. Scuderi, J. Psikal, M. Kucharik, M. De Marco, J. Cikhardt, E. Krousky, Z. Kalinowska, T. Chodukowski, G. A. P. Cirrone, G. Korn, Proton acceleration driven by a nanosecond laser from a cryogenic thin solid-hydrogen ribbon, Phys. Rev. X 6 (2016) 041030. doi:10.1103/PhysRevX.6.041030.
URL https://link.aps.org/doi/10.1103/PhysRevX.6.041030

[48] S. Li, A. Pasc, V. Fierro, A. Celzard, Hollow carbon spheres, synthesis and applications – a review, J. Mater. Chem. A 4 (2016) 12686–12713. doi:10.1039/C6TA03802F.
URL http://dx.doi.org/10.1039/C6TA03802F